CYBERNETICS AND PHYSICS, VOL. 8, NO. 3, 2019, 153–160

MULTIDIMENSIONAL GENERALIZATION OF PHYLLOTAXIS

Andrei Lodkin
Dept. of Mathematics & Mechanics
St. Petersburg State University
Russia
alodkin@gmail.com

Article history:
Received 28.10.2019, Accepted 28.11.2019

Abstract

The regular spiral arrangement of various parts of biological objects (leaves, florets, etc.), known as phyllotaxis, could not find an explanation during several centuries. Some quantitative parameters of the phyllotaxis (the divergence angle being the principal one) show that the organization in question is, in a sense, the same in a large family of living objects, and the values of the divergence angle that are close to the golden number prevail. This was a mystery, and explanations of this phenomenon long remained "lyrical". Later, similar patterns were discovered in inorganic objects. After a series of computer models, it was only in the XXI century that the rigorous explanation of the appearance of the golden number in a simple mathematical model has been given. The resulting pattern is related to stable fixed points of some operator and depends on a real parameter. The variation of this parameter leads to an interesting bifurcation diagram where the limiting object is the $SL(2,\mathbb{Z})$-orbit of the golden number on the segment [0,1].

We present a survey of the problem and introduce a multidimensional analog of phyllotaxis patterns. A conjecture about the object that plays the role of the golden number is given.

Key words

Phyllotaxis, golden number, Diophantine approximation, Klein sail.

1 Introduction. How do Plants Know the Golden Number?

We begin with a small talk about botany, but it is only to start, as we will see in the sequel: the article is mostly about mathematics.

It has been known for several centuries that the arrangement of plant organs, e.g., leaves or branches around a stem, seeds on a pine cone or a sunflower head, florets, petals, scales, and other units usually shows a regular character, see the pictures below.

Figure 1. Spirals on the sunflower head and the marguerite flower.

This phenomenon attracted such scientists as Leonardo da Vinci (XV century), Johannes Kepler (XVI century), Johann Wolfgang von Goethe (XVIII century). The latter was not only a poet, but he also was

involved in a natural science, especially in morphology (the latter term was invented by him) and anatomy of plants and animals.

Phyllotaxis (ancient Greek: "phýllon" means "leaf", and "táxis", "arrangement") is a phenomenon of leaf (and other plant elements) arrangement. There is a variety of phyllotaxy patterns among plants, but only two of them prevail. One of them, in which leaves around the stem, or florets in a daisy flower, etc. are arranged in *spirals* (see Fig. 1, 2), is the most widespread and at the same time intriguing. This type of phyllotaxy was described in detail by brothers Bravais [Bravais & Bravais, 1837], D'Arcy Thompson [Thompson, 1917], and by many others in the XX century.

Figure 2. Spirals on the stem of New Zealand's national symbol: the fern tree.

The other one, *the whorled phyllotaxis* (example: pine or araukaria branches), is more comprehensible. In the latter type of phyllotactic pattern, the leaves are arranged, for instance, in triplets: a triplet of leaves at each level (one can see, on other plants, 2, or 4, etc. leaves at each level). In Fig. 3, you can see that triples are turned at approximately 60° one against another (and this lets more light for leaves).

In the spiral pattern, one can usually see two families of parallel spirals: the members of one family turn clockwise, the members of the other counter-clockwise.

If you count the numbers of spirals in both families, you usually get a pair of numbers like this: 3 and 5, 5 and 8, 8 and 13, etc., these pairs are the pairs of consecutive Fibonacci numbers (f_n, f_{n+1}) of the series 1,1,2,3,5,8,13,21,34,... where $f_{n+2} = f_{n+1} + f_n$. We will say in this case that the species in question obey the (f_n, f_{n+1}) phyllotaxy pattern. As is well known, the sequence of ratios f_n/f_{n+1} tends to *the golden number* $\varphi = \frac{\sqrt{5}-1}{2} = 0.618033\ldots$. There exist, in nature, species with (f_n, f_{n+1})-phyllotaxis where n is rather large, for example, you can encounter even the $(133, 244)$ pattern on a good sunflower head, with $\frac{133}{244} = 0.618025\ldots$. One can get much surprised and seek an explanation of how do plants "know" the golden number with such a good accuracy!

As we will see, there is no mysticism in this phenomenon, nor must an intricate biological mechanism be involved in the explanation: a very simple geometric model can give an answer.

Figure 3. Whorled phyllotaxis: leaves are arranged in triplets: a triplet of leaves at each level.

2 Description of the Phyllotaxis Phenomenon

Here we present a simple model that mimics the phenomenon of the spiral phyllotaxis on a stem and introduce some notions that will be later used in the explanation of the phenomenon.

2.1 Cylindrical Model

In this model, the stem is represented by a semi-cylinder, whereas leaves, branches, and other morphological units are represented by points on its surface. The thing is that these units are very small at the stage when they appear. We formulate a rule according to which these points are being placed, one by one. The author used this model [Lodkin, 1987] in his early computer experiments, as well as the authors of [Levitov, 1991; Douady & Couder, 1992a; Douady & Couder, 1992b] et al.

We take the semi-cylinder $\mathbb{T} \times [0, \infty)$, with $\mathbb{T} = \mathbb{R}/\mathbb{Z}$ a circle, and consider a sequence of its points $\vec{p}_k = (2\pi x_k,\ h_k), k \in \mathbb{N}, x_k \in [0, 1), h_k \geq 0$. The number k has the meaning of the age of the unit (primordium). The vertical step $h_{k+1} - h_k$ is called *the internodal distance*, the difference $\alpha_k = x_{k+1} - x_k \mod 1$ *the divergence angle*, see Fig. 4.

Usually it turns out that the divergence angle and the internodal distance are almost constant. This makes

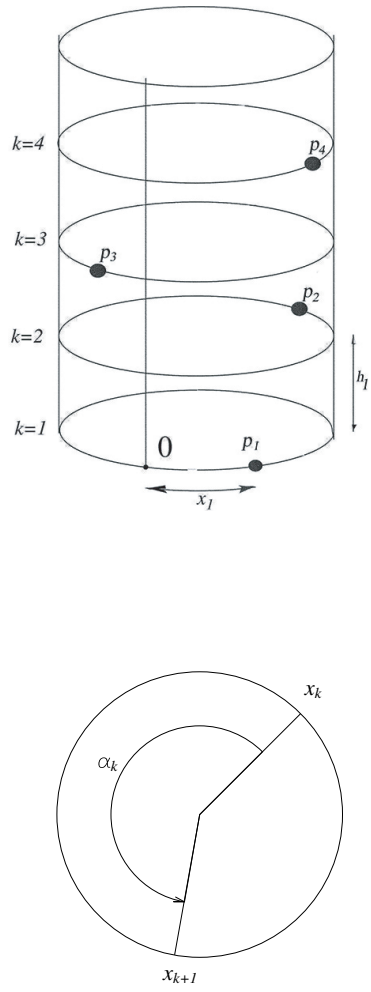

Figure 4. Cylindrical model.

us assume that the vertical coordinates h_k constitute an arithmetic progression $h_k = hk$, and the angular coordinates $x_k = xk \mod 1 = \{xk\}$ are the fractional parts of an arithmetic progression.

We use this model in Subsection 2.6 where we explain the rule of placing points and discuss the effect. In a real plant, the coordinates h_k do not have much significance (except at an early stage) because the internodal distance constantly increases (the so-called intercalar growth) while the plant grows, whereas the divergence angle usually stabilizes to some limit x that characterizes the phyllotaxy pattern. The remarkable fact is that in most cases x is close to the golden mean φ or, rarely, to some number of the form $\frac{a\varphi+b}{c\varphi+b}$, where $a, b, c, d \in \mathbb{Z}, ad - dc = 1$. In the latter case we say that $x = g(\varphi)$, where $g = \left(\begin{smallmatrix} a & b \\ c & d \end{smallmatrix}\right)$ is an element of $SL(2, \mathbb{Z})$, the group of integer matrices with determinant 1.

2.2 Accompanying Lattice

The set of points

$$L^0_{x,h} = \{\vec{p}_k = (kx \mod 1, kh) \mid k \in \mathbb{N}\} \subset [0,1) \times \mathbb{R}_+$$

corresponding to the phyllotaxis with constant parameters x and h forms a lattice on the cylinder whose development on the plane we represent by the strip $[0,1] \times \mathbb{R}_+$ with two border lines identified (Fig. 5). This lattice can be extended to the full lattice

$$L_{x,h} \subset \mathbb{R}^2$$

with basis consisting of two vectors $\vec{u} = \vec{p}_1 = (x, h)$ and $\vec{v} = (1, 0)$. In other words,

$$L_{x,h} = \{m\vec{u} + n\vec{v} \mid m, n \in \mathbb{Z}\}.$$

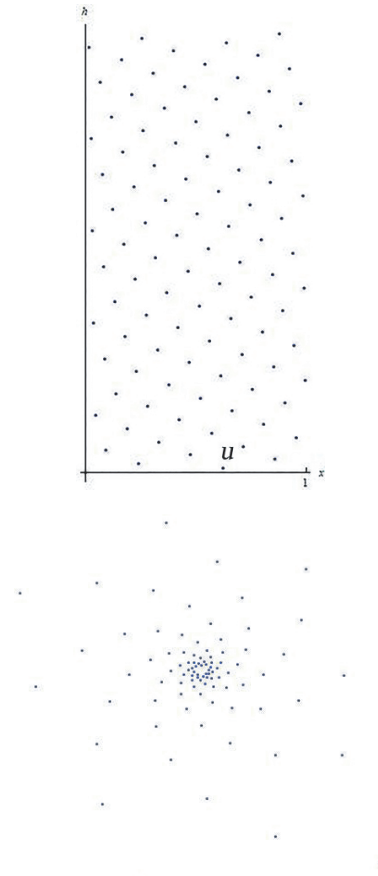

Figure 5. Lattice $L^0_{x,h}$ and its disk image.

2.3 Disk Model

A similar representation of the phyllotaxis such as one to be observed in a daisy flower or in a sunflower head may be obtained on the disk $x^2 + y^2 \le 1$ if we take the images of the points $\vec{p}_k$ under the mapping

$$(x_k, h_k) \mapsto (e^{-h_k} \cos 2\pi x_k, e^{-h_k} \sin 2\pi x_k),$$

or, in the complex presentation,

$$z_k = 2\pi x_k + ih_k \mapsto \exp(iz_k).$$

The center of the disk corresponds to the infinity on the cylinder.

Simple transformations can also send one of the patterns above to a pattern on the geometrical cone that is a model of a pine or spruce cone.

2.4 Parastichies

In the cylindrical model, the *parastichies* (the Greek "para" means "near", and "stixos", row) are imaginary straight lines passing through lattice points. The indices (= birth dates) of points in one parastichy form a progression

$$P_{m,k} = m\mathbb{N} + k = \{m + k, 2m + k, 3m + k, \dots\}.$$

Given positive integer $m \in \mathbb{N}$, one obtains m such parallel parastichies for $k = 0, \dots, m - 1$.

The best discernible parastichies form two families:

m parastichies going clockwise around the stem and

n parastichies going anticlockwise.

This pattern is called the (m, n)-phyllotaxis.

It should be noted that all points of the lattice $L^0_{x,h}$ belong to a single line (corresponding to a cylindrical spiral) called *the generative spiral* which is usually difficult to see when h is small because its inclination is very small.

In the disk model, all parastichies look like spirals.

If one continuously changes h leaving x fixed, he will see that the most discernible parastichies go and come: one pair disappears, another becomes visible.

There is a simple rule that translates the divergence angle x into the series of parastichy numbers pairs (m, n) that appear while h decreases from ∞ to 0. Take the development of x into a continued fraction

$$x = [0; a_1 a_2 a_3 \dots] = \cfrac{1}{a_1 + \cfrac{1}{a_2 + \cfrac{1}{a_3 + \dots}}}$$

and consider its rational approximations (convergents)

$$r_i = [0; a_1 \dots a_i] = \frac{p_i}{q_i}.$$

Then the pairs of parastichies that are visible at the convenient values of h are the pairs $(m, n) = (p_i, q_i),\ i = 1, 2, \dots$.

Thus, the golden number $\varphi = [0; 1, 1, 1, \dots]$ corresponds to the Fibonacci pairs (f_i, f_{i+1}) as in this case $f_i = [0; \overbrace{1, \dots, 1}^{i}]$, and we come to the sequence of rational convergents of φ:

$$[0; 1] = \frac{1}{1},\ [0; 1, 1] = \frac{1}{2},\ [0; 1, 1, 1] = \frac{2}{3}, \dots .$$

This correspondence gives a practical means to measure the divergence angle on a real biological object in which units are far from being points and it is very difficult to find the consecutive units because chronological neighbors are very far from each other on the cylinder surface. Instead, one can simply count the left and right parastichies and take the ratio $\frac{m}{n}$ as an approximation to x (by the way, a very good one: $|x - \frac{m}{n}| < \frac{1}{n^2}$).

3 Attempts toward Finding an Explanation

Two problems arise:

Why phyllotactic pattern is usually a lattice?
How does a plant know the golden number?

Some researchers tried to find an explanation of the existence of parastichies by looking for morphological relationship between their units. For instance, they were looking for some material links like vessels joining the elements of a parastichy. They do exist sometimes, but they materialize post factum, after the relative position of the primordia is fixed at the early stage of the morphogenesis.

3.1 Global vs local Mechanism

Much more realistic approach was based on the explanation of the regular phyllotaxis from the point of view of better illumination of the whole leaf system of the grownup plant, or some similar factor (the search of global mechanisms).

In more recent time, theories based on local mechanisms of consecutive appearance of the primordia prevail. Local mechanism theories were motivated to a great extent by the study of the pictures of the apex (the top of the growing stem) region made with an electronic microscope (Fig. 6[1]). The character of the appearance of primordia in this area suggested the *geometric* theory, which states that the new primordium seeks for the least crowded place to appear at. The other one, the *diffusion-inhibition* model, is based upon the conjecture that the apex and the existing primordia emits some substance (inhibitor) that is gradually spreading out, and the new primordium is looking for a place with the least concentration of this substance.

3.2 Modeling, Computer Experiments

The geometric model suggests the following algorithm of the appearance of primordia. We take the cylinder mentioned above and place the points at the levels $hk, k = 1, 2, \dots$, one point at each level (h being the parameter of the model). Given the points $\vec{p}_1, \vec{p}_2, \dots, \vec{p}_n$, we put the point $\vec{p}_{n+1}$ at the $(n+1)$th level at such place x_{n+1} that maximizes the minimal distance of the new point from the existing ones. Using this simple scheme,

[1] These pictures are taken from the internet.

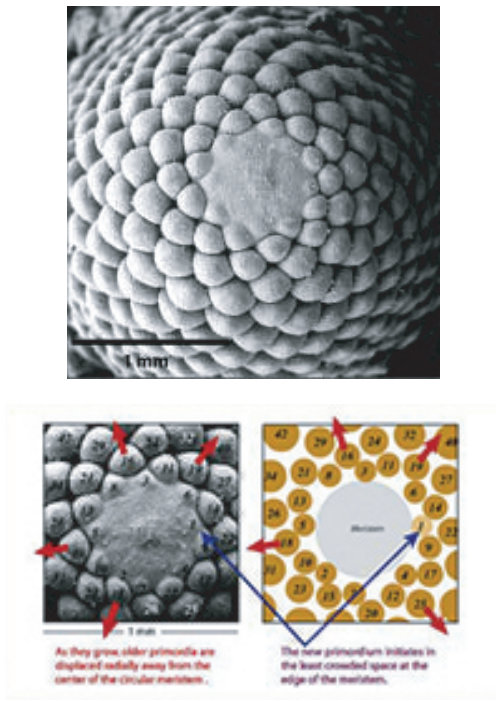

Figure 6. The real apex under the electronic microscope. The numbers mean the age of primordia

in 1986, the author has modeled on a computer the patterns for various values of h and observed that for small values of this parameter, the points $\mathbf{p_k}$ formed a lattice on the cylinder with divergence angle close to 137.5° or 222.5°, that is, $2\pi\varphi$ or $2\pi(1-\varphi)$. Moreover, it was possible on a computer to place the first n points at random, and in 4 or 5 steps the regular lattice pattern reappeared. Later, S. Douady and Y. Couder [Douady & Couder, 1992a; Douady & Couder, 1992b] executed extensive computer simulation with various parameters. In [Smith et al., 2006], computer simulation was based upon the diffusion–inhibition model. It became obvious that a simple mechanism works and the lattice pattern is stable.

3.3 Physical Experiments

More evidence to the fact that the regular phyllotactic picture was due to the reasons more simple than biological ones was brought up when L. S. Levitov [Levitov, 1991] made similar experiments with layered semiconductors. An impressive experiment was made by Douady and Couder. They let magnetic drops gradually, one by one, fall down into the center of a saucer filled with oil. The repulsive force made the drops scatter across the saucer and form patterns resembling the sunflower head.

3.4 Rigorous Results

It comes to one's mind that the lattice arrangement of points minimizes some energy. Assuming this, L. S. Levitov has found the value of the parameter x that minimizes the total energy

$$E = \sum_{i \neq 0} U(||\vec{p}_i - \vec{p}_0||)$$

of the lattice $L_{x,h}$ for the potential $U(d) = d^{-s}$ and various values of the constant parameter h.

P. Atela, C. Golé and S. Hotton [Atela et al., 2002] investigated a dynamical system on the multidimensional torus $\mathbb{T}^{n+1}$ based on local rules. For each h, these authors considered the operator $\mathbb{T}^{n+1} \to \mathbb{T}^{n+1}$. The meaning of this operator is the following. Given the points $\vec{p}_0, \ldots, \vec{p}_n$ at $n+1$ consecutive levels, we move the configuration one level down and put a new point at the nth level that gives minimum distance of the new point from the set of n its predecessors. Passing to the coordinates $y_k = x_{k+1} - x_k \mod 1$ (due to the symmetry of the model), one comes to the operator $\Phi : \mathbb{T}^{n+1} \to \mathbb{T}^{n+1}$ of the form

$$(y_0, y_1, y_2, \ldots, y_n) \mapsto (y_1, y_2, y_3, \ldots, y_n, \phi(y_0, y_1, y_2, \ldots, y_n))$$

where the function ϕ is defined by the y-coordinate of the point $\vec{p}_{n+1}$ optimal in the sense of Subsect. 3.2.

It was shown that the fixed points (vectors) for this operator are constant sequences $X = (x, x, \ldots, x)$ that correspond to the spirals with constant divergence angle $x = x(h)$ and that these fixed points are stable, i.e., if one takes a vector $Y = (y_0, \ldots, y_n)$ with $|y_i - x|$ small enough, then $\Phi^k Y \to X$ as $k \to \infty$.

The two investigations give similar results showing that global optimality can be reached by local optimization.

3.5 Bifurcation Diagram

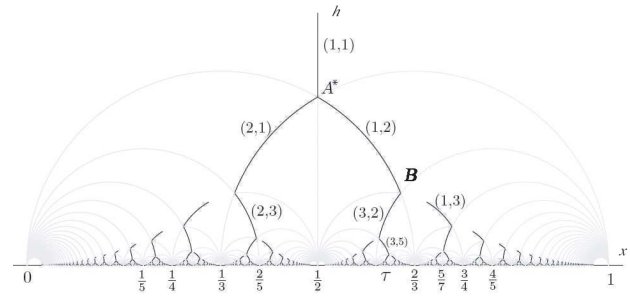

Figure 7. Bifurcation diagram.

The dependence of the stable divergence angle x on the internodal distance h can be represented by the following diagram (Fig. 7)[2]. One sees that when h is big enough,

[2]This diagram appeared in van Iterson's investigation [van Iterson, 1907].

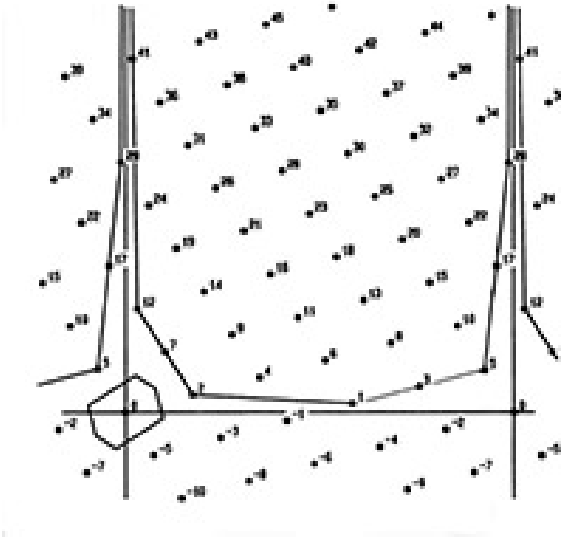

Figure 8. Sail and Voronoï cell.

there is only one option $x = 0.5$: it is clear that the optimal spacing of each new point is right on the opposite side of the cylinder. When h decreases, there is a bifurcation point at some its critical value, after which the optimal point must be displaced either to the right or to the left, and thus the vertical line $x = x(h)$ is replaced with two branches. We say that the *symmetry breaking* of the model takes place: during the further slowing down of h, there comes a series of points where the branches have turning points. It can be shown that at each such point there is no alternative: the system chooses only one of two branches, turning alternatively to the right or to the left [Atela et al., 2002; Bergeron and Reutenauer, 2019; Levitov, 1991].

The meaning of the smooth segments of the diagram is the following. When we move along a segment, the lattice remains such that the most visible parastichies correspond to a (m, n) pattern. For the principal branch marked AB of the diagram, m and n are consecutive Fibonacci numbers: (1,1), then (1,2), (2,3), (3,5), and so on. The vertices of the broken line correspond to the pattern change. This change is due to the fact that points of the lattice which were distant at the parameter value corresponding to one segment become close at smaller values of h. This broken line approaches the point φ on the $h = 0$ axis.

3.6 Sail and Diophantine Approximation

Originally, the *Klein polygon* (see, e.g., [Arnold, 2001; Korkina, 1995; Karpenkov, 2004]) is the convex hull of the intersection of a lattice with a quadrant on the plane, and the *sail* is its border. Due to periodicity and central symmetry of the lattice $L_{x,h}$ (Subsect. 2.2), we see that the intersection of $L_{x,h}$ with a half-stripe $(n, n+1)\times\mathbb{R}_+$ does not depend on $n \in \mathbb{Z}$. Taking $n = 0$, we come to $L^0_{x,h}$. Call the border of its convex hull the sail again. If x is irrational, no point of the sail lies on the border of the half-stripe, so the sail is an infinite broken line whose vertices are the points $\vec{p}_k = (kx \mod 1,\ kh)$ for some $k \in \mathbb{N}$.

Now we focus on these numbers k. Recall the sequence $r_i = p_i/q_i$ of convergents of the continued fraction expansion $x = [0; a_1a_2a_3\dots]$ of the real number x. The numbers p_i, q_i are exactly the indices k of the vertices $\vec{p}_k$ of the sail approaching the ray $0 \times \mathbb{R}_+$ in turns from the left and from the right. In Fig. 8, these k are the numbers 1,2,5,12,29,70,.... The elements a_i of the continued fraction are well seen on the sail: they are the so-called integer lengths of the segments of the broken line. This means that a_i is the number of points of the lattice that lie on the ith segment, minus 1. For the sail corresponding to $x = 0.70707\cdots = [0; 12222\dots]$ in Fig. 8, we have $a_1 = 1$ (the segment $[\vec{p}_1, \vec{p}_2]$ contains two lattice points), $a_2 = 2$ (the segment $[\vec{p}_1, \vec{p}_5]$ contains three lattice points), $a_3 = a_4 = a_5 = 2$, and so on, and the rational convergents r_i are $1, \frac{2}{5}, \frac{5}{12}, \frac{12}{29}, \frac{29}{70}, \dots$.

The lattice points can have more or less uniform distribution, and the degree of uniformity is in close relation with the form of the *Voronoï cell* that is the polygon centered at some point of the lattice, say, $\vec{p}_0 = \vec{0}$, consisting of the points of the plane that are closer to the center than to any other point of the lattice. The more protruded is this cell, the less uniform is the lattice. Conversely, the closer the cell to a disk, the more uniform (in a sense we do not want to precise here), or isotropic, or good looking is the lattice, see Fig. 9. It is known that in the one-dimensional case the most uniform (or low-discrepancy) filling of the unit interval by the points $kx \mod 1, k = 1,\dots n$ is attained at $x = \varphi$. It is possible that similar two-dimensional sequences can be found among the lattices $L^0_{x,h}$.

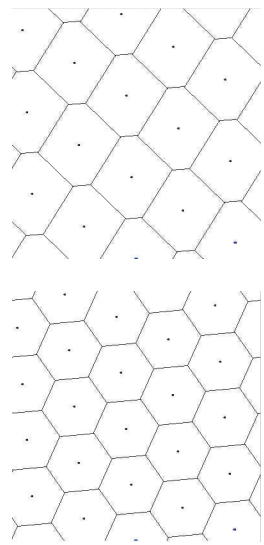

Figure 9. The Voronoï cells for a random and the golden lattices.

Now we can say how to describe in what sense the lattices corresponding to the golden number are the optimal ones.

Let us watch how the Voronoï cell $V = V(x,h)$ behaves when we vary h keeping x fixed. Let Γ be the border of V. We call the asphericity of V the number

$$A(V) = \frac{\max\{||t|| \;\big|\; t \in \Gamma\}}{\min\{||t|| \;\big|\; t \in \Gamma\}}.$$

It can be shown that the variation of $A(V)$ while h tends to 0 is minimal when $x = \varphi$ or $1-\varphi$. This means that V remains to be a hexagon which is close to the regular one during the whole variation of the internodal distance h as compared to other values of x, and the alternating most visible parastichies keep being most isotropic, i.e., they intersect each other at the angle that is not far from 60°. In terms of the sail, this means that the integer lengths of the broken line (the border of the sail) are the minimal ones: all equal to 1 (recall that $\varphi = [0;1,1,1,\dots]$). It is known in the Diophantine approximation theory that φ is the real number the worst approximated by rational numbers. See [Lodkin, 2019] for a more detailed exposition of the relation between sail geometry and Diophantine properties of x in terms of the so-called *cardiogram* of x. In [Bergeron and Reutenauer, 2019], a similar characteristic of the bad approximation, in terms of the "growth function", is given.

4 Multidimensional Generalizations

Here we present an analog of the phyllotaxy theory in higher dimension.

4.1 Cylindrical Model

Instead of the circle, we take a multidimensional torus

$$\mathbb{T}^n = \mathbb{R}^n/\mathbb{Z}^n, n \in \mathbb{N},$$

with flat metric

$$d(\vec{x},\vec{y}) = \text{dist}(\vec{x},\vec{y}+\mathbb{Z}^n) = \min\{||\vec{x}-\vec{y}+\vec{k}|| \mid \vec{k} \in \mathbb{Z}^n\}.$$

In $\mathbb{R}^{n+1} = \mathbb{R}^n \times \mathbb{R}$, consider the half-cylinder

$$C = \mathbb{T}^n \times [0,+\infty).$$

also with natural flat metric. For a positive real h, one can construct a sequence of points $\vec{p}_k \in C$ as follows (cf. Subsect. 3.2). Given the points $\vec{p}_k = (\vec{v}_k, kh), k = 0,\dots,m$, with $\vec{v}_k \in \mathbb{T}^n$, take $\vec{p}_{m+1}$ to be the point that minimizes the distance from $\vec{p}_{m+1}$ to the set $\{\vec{p}_0,\dots,\vec{p}_m\}$. One can start with one point, say, $\vec{v}_0 = \vec{0}$, or with any finite number of points, and construct a sequence following this rule. It is clear that the position of the point $\vec{p}_{m+1}$ on the $(m+1)$th level is determined by not more than $\frac{\sqrt{n}}{2h}$ predecessors.

We can outline a plan and set up a number of conjectures.

Conjecture 1. As in the case $n = 1$, the vectors $\vec{v}_{k+1} - \vec{v}_k$ tend to some limit $\vec{v} = \vec{v}(h)$ (the constant *divergence vector*).

Question 1. What are the possible such $\vec{v}$, for each h? How does the analog of van Iterson's diagram look like?

Let $L^0_{\vec{v},h} = (\{\vec{p}_k = k\vec{v} \mod \mathbb{Z}^n), kh \mid k \in \mathbb{Z}_+\} \subset C$ be the lattice generated by the vector $\vec{v} \in \mathbb{R}^n$.

Question 2. What are the optimal lattices in the energetic sense (cf. Subsect. 3.4)?

Question 3. What vectors are the limits of the principal branches of the bifurcation diagram as $h \to 0$?

In the case $n = 2$, we have a candidate for such a vector. Its choice is motivated by the relation, in the one-dimensional case, between geometrical properties of the lattices $L^0_{x,h}$ and Diophantine properties of the number x, and the hope this relation persists in higher dimension.

In the author's work with his former student S. M. Bliudze, this relation was explored in dimension 2.

Theorem ([Bliudze, 1998], unpublished) *The worst approximated (in some precise sense) vector in $\mathbb{R}^2$ is $\vec{v}_\psi = (\psi,\psi^2)$, where $\psi = 1.3247\dots$ is the real root of the polynomial $x^3 - x - 1$ (the plastic number).*

The notion of the cardiogram (see Subsect. 3.6) is defined in an arbitrary dimension. In the case of the family of lattices $\{L^0_{\vec{v},h}, h > 0\}$, this characteristic is presumably extremal for $v = v_\psi$ (cf. φ and its cardiogram). Anyway, these vector and corresponding lattices attract one's attention in some other aspects. For instance, this family of lattices is interesting in what concerns discrepancy, or the question on the most evenly-distributed sets of points, cf. [Schretter et al., 2011].

Now we can reverse the direction **nature** → **math** to **math** → **nature** and ask the question: **Is there an object in nature (e. g., a sort of fruit) that corresponds to our $L^0_{\vec{v}_\psi,h}$ lattice?**

4.2 Compact Model

Like in Subsect. 2.3, we can transform the lattice in the half-cylinder C into the lattice in the compact domain D. This can be done, for example, as follows: $T(x,y,h) = (X,Y,Z)$, where

$$\begin{aligned} X &= (1 + 0.5e^{-h}\cos 2\pi x)\cos 2\pi y,\\ Y &= (1 + 0.5e^{-h}\cos 2\pi x)\sin 2\pi y,\\ Z &= 0.5e^{-h}\sin 2\pi x. \end{aligned}$$

Here D is a toric body, and the images of the lattice condense around the circle $X^2 + Y^2 = 1, Z = 0$ (see Fig. 10).

Another transformation with

$$\begin{aligned} X &= e^{-h}(1 + \cos 2\pi x)\cos 2\pi y,\\ Y &= e^{-h}(1 + \cos 2\pi x)\sin 2\pi y,\\ Z &= e^{-h}\sin 2\pi x \end{aligned}$$

effectuates a one-point compactification of the half-cylinder. In this case the images of the lattice points condense around the origin (see Fig. 11).

These "3D-fruits" may be considered as analogs of a sunflower head.

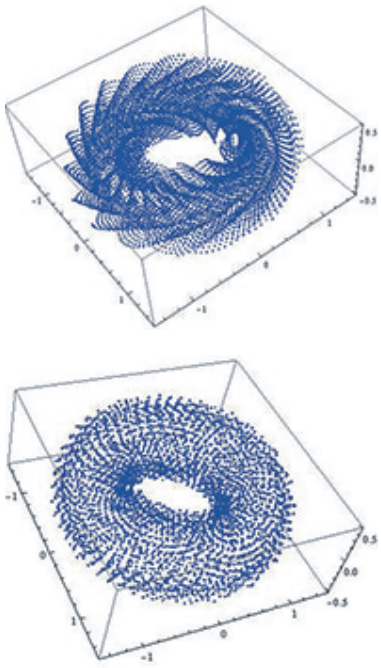

Figure 10. The toric images of a random and the platinum 3D-lattices.

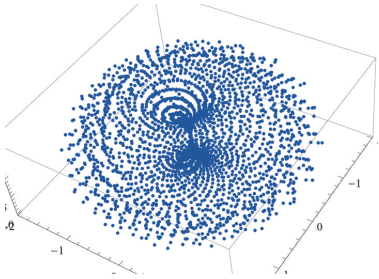

Figure 11. The image of the platinum lattice in the 1-pt compactification.

5 Conclusion

We sketched an introduction to multidimensional phyllotaxy theory and its possible connections with Diophantine approximation of vectors, lattices of least energy, discrepancy theory in higher dimension, et al. which will be extended in forthcoming publications. Also, we suggested a 2D-analog of the golden number.

6 Acknowledgements

This work has been supported by the RFBR, grant No. 17-01-00433.

References

Arnold, V. I. (2001). *Continued Fractions.* Moscow.

Atela, P., Golé, C., and Hotton, S. (2002). A dynamical system for plant pattern formation: a rigorous analysis, *J. Nonlinear Sci. Vol.* **12**(6).

Bergeron, F., and Reutenauer, C. (2019). Golden ratio and phyllotaxis, a clear mathematical link. *Journal of mathematical biology*. **78**(1-2), 1–19.

Bliudze, S. M. (1998). *Optimal continued fractions.* Master thesis. St. Petersburg State University (in Russian).

Bravais L., Bravais A. (1837). Essai sur la disposition des feuilles curvisériées. *Ann. Sci. Nat.*(2) **7**, 42-110, 193-221, and 291–348.

Douady, S., and Couder, Y. (1992). Phyllotaxis as a physical self organised growth process. *Phys. Rev. Lett.* **68**, 2098–2101.

Douady, S., and Couder, Y. (1996). Phyllotaxis as a dynamical self organizing process. Part I. The spiral modes resulting from time-periodic iterations. *J. Theor. Biol.* **178**, 255–274. Part II. The spontaneous formation of a periodicity and the coexistence of spiral and whorled patterns. Ibid, 275–294. Part III: The simulation of the transient regimes of ontogeny. Ibid, 295–312.

Van Iterson, G. (1907). Mathematische und microskopisch-anatomische Studien ber Blattstellungen, nebst Betrachtungen ber den Schalenbau der Milionen, Verlag von Gustav Fischer in Jena.

Karpenkov, O. N. (2004). Two-dimensional continued fractions of hyperbolic integer matrices with small norm. *Russian Mathematical Surveys* **59**(5), 959–960.

Khinchin, A. Ya. (1935). *Continued Fractions.* Mineola, N.Y.Dover Publications, 1997 (first published in Moscow, 1935).

Korkina, E. I. (1995). Two-dimensional continued fractions. The simplest examples. (Russian) *Trudy Mat. Inst. Steklov.* **209**, Osob. Gladkikh Otobrazh. s Dop. Strukt., 143–166.

Levitov, L. S. (1991). Phyllotaxis of flux lattices in layered superconductors. *Phys. Rev. Lett.* **66**, 224–227.

Lodkin, A. A. (1987). Mathematical modelling of phyllotaxis. In: *V-th All-Union School on Theoretical Morphology of Plants*. Lvov, 59–65 (in Russian).

Lodkin, A. A. (2019). Klein sail and Diophantine approximation of a vector. Zap. Nauchn. Sem. S.-Peterburg. Otdel. Mat. Inst. Steklov. (POMI) **48**, 63-73 (in Russian). English version to appear in *Journal of Mathematical Sciences* (New York), 2020.

Schretter, C., Kobbelt, L., Dehaye, P.-O. (2011). Golden ratio sequences for low-discrepancy sampling. *Journal of Graphics Tools*, **16**(2), 95–104.

Smith, R. S., Kuhlemeier, C., and Prusinkiewicz, P. (2006). Inhibition fields for phyllotactic pattern formation: a simulation study. C*anadian Journal of Botany*, **84**(11), 1635–1649.

Thompson, D'Arcy W. (1917). *On Growth and Form.*